THE PHYSICAL BASIS OF Lg GENERATION BY EXPLOSION SOURCES

Jeffry L. Stevens[1], G. Eli Baker[1], Heming Xu[1], Theron J. Bennett[1], Norton Rimer[1], and Steven M. Day[2]

Science Applications International Corporation[1], San Diego State University[2]

Sponsored by National Nuclear Security Administration
Office of Nonproliferation Research and Engineering
Office of Defense Nuclear Nonproliferation

Contract No. DE-FC03-02SF22676[1, 2]

ABSTRACT

The goal of the project is to develop a quantitative predictive capability for explosion-generated Lg phases with a sound and unambiguous physical basis. The research program consists of a theoretical investigation of explosion-generated Lg combined with an observational study. The specific question addressed by this research program is how the Lg phase is generated by underground nuclear explosions. This question is fundamental to how Lg phases are interpreted for use in explosion yield estimation and earthquake/explosion discrimination.

A simple point explosion in an infinite medium generates no shear waves, so the Lg phase is generated entirely by nonspherical components of the source and conversions through reflections and scattering. We find that the most important contributors to the Lg phase are (1) P to S conversion at the free surface and other near source interfaces; (2) S waves generated directly by a realistic distributed explosion source, including nonlinear effects resulting from the free surface and gravity; and (3) Rg scattering to Lg. Additional effects that contribute to Lg are the scattering of converted S phases that traps more of the converted P to S in the crust, and randomization of the components of Lg.

We analyze several explosion data sets: (1) Degelen Mountain explosions recorded at distances less than 100 km and corresponding recordings at Borovoye (BOR) at 650 km; (2) recordings from Russian deep seismic sounding experiments; (3) Nevada Test Site (NTS) explosion sources including the Nonproliferation Experiment (NPE) and nuclear tests covering a range of source depths and media properties. Using the NTS data, we are investigating the dependence of three-component Lg amplitudes and spectra on source depth and media attributes (including gas porosity), to complement the model predictions.

We model the overburied NPE, and underburied and overburied Degelen explosions, using point sources and two-dimensional nonlinear finite-difference calculations to quantify the source effects. Finite-difference calculations indicate that the topography at Degelen much more effectively scatters P and Rg to Lg, and traps more of the surface P-to-S converted phase in the crust, than do crustal heterogeneities. We use energy conservation to determine an upper bound on Rg to Lg scattering. Rg to Lg scattering may contribute to Lg and Lg coda at frequencies less than 1 Hz, but contributes less at higher frequencies than Lg generated directly by the explosion or by surface P-to-S conversion.

OBJECTIVES

The goal of the project is to develop a quantitative predictive capability for explosion-generated Lg phases with a sound and unambiguous physical basis. The research program consists of a theoretical investigation of explosion-generated Lg combined with an observational study. The specific question addressed by this research program is how the Lg phase is generated by underground nuclear explosions. This question is fundamental to how Lg phases are interpreted for use in explosion yield estimation and earthquake/explosion discrimination.

RESEARCH ACCOMPLISHED

A simple point explosion in an infinite medium generates no shear waves, so the Lg phase is generated entirely by nonspherical components of the source and conversions through reflections and scattering. The most important contributors to the Lg phase are (1) P-to-S conversion at the free surface and other near-source interfaces, (2) S waves generated directly by a realistic distributed explosion source including nonlinear effects as a result of the free surface and gravity, and (3) Rg scattering to Lg. In addition to source and near source effects, Lg is affected by scattering and conversion along the travel path. The most important effects are S-to-S scattering that changes the orientation and direction of the near source P-to-S converted waves, affecting the extent to which they are trapped in the crust and randomization of the components of Lg, although the calculations presented in this study suggest that topographic scattering of P-to-S converted waves may be more important. The focus of the project is to quantify through data analysis and simulations the dependence of these various mechanisms on source conditions. We have made considerable progress in understanding explosion-generated shear waves by quantifying and numerically reproducing features of observations of shear waves generated under different source conditions.

In the proceedings paper for the first year of this project (Stevens et al., 2003), we described the data sets collected, their analysis, and the results of nonlinear finite difference simulations of explosion sources under different source conditions. We briefly review those results, adding some new results to the observations.

Table 1 lists the data sets, which provide waveforms from explosions ranging from 100s of meters from the source to regional distances. Table 2 lists the most important new observations from the project. There are three principal conclusions that can be drawn from the observations: (1) There is strong evidence for shear waves generated directly by the source that are observable at regional distances; (2) there is strong evidence for transverse Lg generated directly by or very close to the source that cannot be explained by a spherically symmetric explosion, a vertically oriented Compensated Linear Vector Dipole (CLVD), or any other axisymmetric source; and (3) the Rg phase persists to great distances in some earth structures, notably Central Asia.

These observations show that S is generated directly by the source and is observable in local records and that the explosion generates an impulsive Sn phase and will therefore also generate Lg. Lg due to Rg scattering may be superimposed on this signal. A major objective of our project is to determine the relative sizes of these components of Lg. The persistence of Rg in Eurasia suggests that the scattering rate there may be quite different from the western United States.

Table 1. Data Collected and Used in the Current Project.

Source	No. Events	Yield, Depth, or mb range	Recording Range
Degelen	7	1.5–78 Kt	7-50 km & 650 km
Deep Seismic Soundings (DSS)	4	8.5–22 Kt	every 10–15 km for 1000s of km in two directions
NTS	155	111–701 m depth	190–400 km
NPE	1	1 Kt 400 m depth	65 near source (100s of m), 3 local, 60 regional (10s-100s of km)
Khirgizia (decoupling)	4	1–6 tons 292 m depth	5–10 km
Lop-Nor	10	4.7–6.4 mb	250–1900 km
Balapan	21	4.8–6.1 mb	950–1500 km

Table 2. Summary of Observations and Their Implications.

Observations	Implications
Sg (tangential and radial) is observed very near the source for the NPE, Deep Seismic Sounding (DSS) profiles, and Degelen explosions.	Some shear waves, both SH and SV, must be generated at or very near (within 100s of meters of) the source.
Rg persists to hundreds of km in the DSS data.	The rate of Rg scattering and attenuation in Eurasia are very different from the Western U.S. and this may reduce Lg generated by Rg scattering.
Distinct impulsive Sg and Rg are clearly separate at a few km to 100s of km from Degelen and DSS explosions.	Temporally compact shear waves are generated independent of Rg scattering for many of the data sets.
Shear wave phases are usually larger on horizontal than vertical seismograms.	Additional relevant information about the explosion source is contained in the horizontal component of Lg.
Sn is prominent, short duration, and sharp for Degelen explosions recorded at BOR.	Sharp Sn is consistent with generation at or very near the source and inconsistent with a distributed scattering process.

Stevens et al. (2003) focused on observations and source calculations. In this paper we focus on further source calculations and two types of scattering calculations. These calculations provide a means of investigating the relative importance of the proposed mechanisms under different source and near-source conditions. Finite-difference scattering calculations show the effects of topography and heterogeneity on P-to-S and Rg-to-S scattering and trapping of the scattered S in the crust. A modal method is used to place an upper bound on Rg-to-Lg scattering and characterize the frequency and temporal dependence of its contribution.

Nonlinear finite-difference source calculations: Figure 1 shows Lagrangian finite-difference near source calculations of a 62 kt explosion in a high-velocity medium at depths of 300 and 1,000 meters (75 and 252 m/kt$^{1/3}$), which are underburied and overburied, respectively, compared to a standard containment depth of approximately 120 m/kt$^{1/3}$. For the shallow explosion, the region of nonlinear deformation is more conical than spherical, but for the deep explosion, the primary region of deformation around the explosion is approximately spherical, but there is an additional region of spall and similar nonlinear behavior near the free surface. The deeper explosion therefore generates a smaller direct-S phase and smaller Lg. These differences suggest that this effect could be observable in Lg from deep explosions in high-velocity media; however, none of the Degelen explosions were this deep.

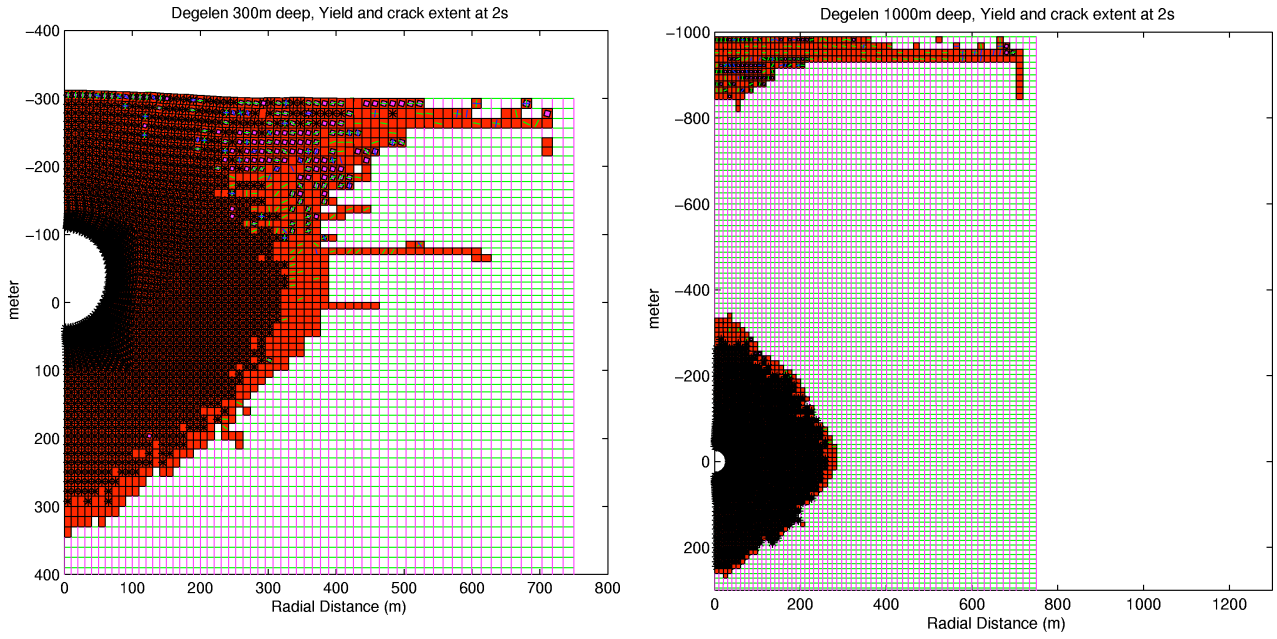

Figure 1. Regions of nonlinear yielding and cracking from an explosion in a high-velocity structure similar to the Degelen test site. Left – 62 kt at 300 meters depth. Right – 62 kt at 1,000 meters depth.

Effects of topography and heterogeneity on free-surface P-to-S scattering: To investigate P-to-S and Rg-to-Lg scattering, we compare results of finite-difference calculations for 5 models, using a point-explosion source at 325 m depth. The first is a homogeneous, horizontally layered velocity model appropriate for Degelen Mt (Figure 2, left side). The second model is that base model plus the topography at Degelen Mt. (Figure 2, second from left). It uses a topographic profile along an east-west line through Degelen, while maintaining the average upper layer thickness. The third model is the base model plus zeroth order Von Karman-distributed P- and S-wave velocity variations with a 5% standard deviation, an aspect ratio of 1, and a correlation length of 1 km in the upper 1.5 km (Figure 2, center). The correlation length corresponds to the Rg wavelength in the passbands of interest and so should effectively scatter it. The fourth model combines the topography and upper layer heterogeneity (Figure 2, second from right). The fifth model adds heterogeneity throughout the crust to the fourth model. The heterogeneities below the surface layer also have a 5% standard deviation, but are asymmetric with a 5:1 horizontal-to-vertical aspect ratio. This last model is intended to test whether additional, surface-converted, P-to-S wave energy can be trapped by scattering induced changes in incidence.

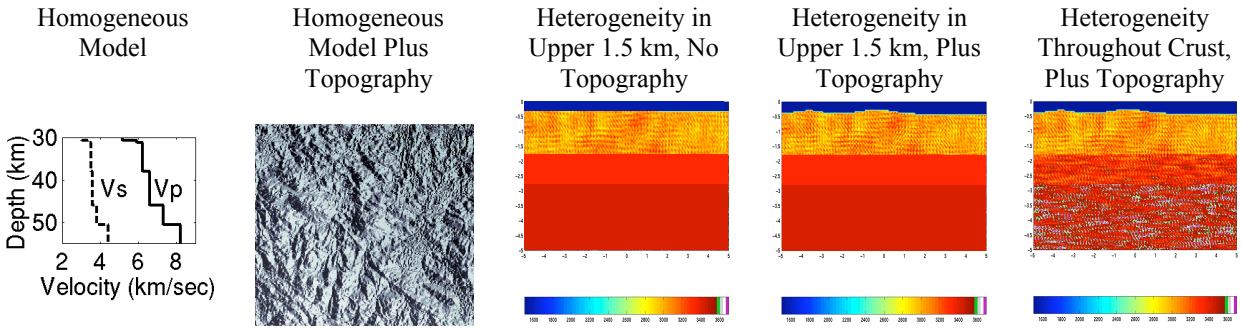

Figure 2. Models used in the scattering calculations. The far left plot shows the 1D homogenous base model. The second plot shows a 200 x 200 km shaded relief image centered on Degelen Mt. The next 3 plots show 5 km deep by 10 km wide slices of the heterogeneous models described in the text. The source is always 325 m deep, and its position for the models with topography is in the center (horizontally) of the snapshots shown.

Figure 3 shows the effects of topography and heterogeneity on the seismograms. Each record section's position corresponds to the position in Figure 2 of the model used to generate the data. The source P-wave velocity is greater than the upper mantle S-wave velocity, so in the base model where there is no scattering that will change the wavenumber, the energy in pS (the free surface P-to-S converted phase) is expected to propagate into the mantle. There is some Sg or Lg seen in the base model record section, however (Figure 3, left side), caused primarily by the non-geometric P-to-S scattered phase S* (e.g., Vogsfjord, 1997), which we address in the discussion of Figure 6. For the model with topography, the Sg or Lg phase is more prominent, indicating that the incidence of pS is sufficiently randomized by the irregular free surface so that some is now trapped in the crust (Figure 3, second from left). Adding heterogeneity to just the surface layer makes little difference to pS (Figure 3, center). The record section for the fourth model also looks much like that of the second. That is, adding surface layer heterogeneities to the model with topography changes little in the records. The addition of heterogeneity throughout the crust causes an increase in coda throughout the records but does not appear to amplify Lg.

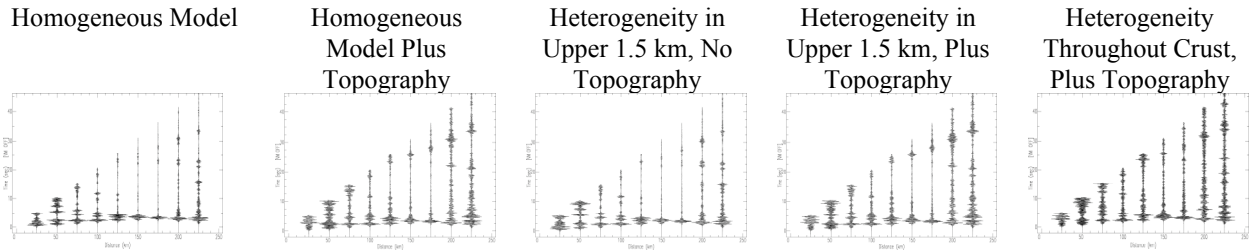

Figure 3. Radial record sections for a 325-m depth point explosion filtered from 3 to 5 Hz, from 25 to 225 km.

Figure 4 shows just the Lg windows at 225 km, filtered from 3 to 5 Hz, for each model. These are the most distant traces of each record section in Figure 3. The rms amplitudes of the Lg phases corrected for pre-Lg noise levels,

listed to the left of the radial traces and right of the vertical traces, are given as a percent of the rms Lg amplitude for the homogeneous model with topography added. The rms Lg amplitude is larger for the models with topography, and topography appears to be the most important factor in trapping pS in the crust.

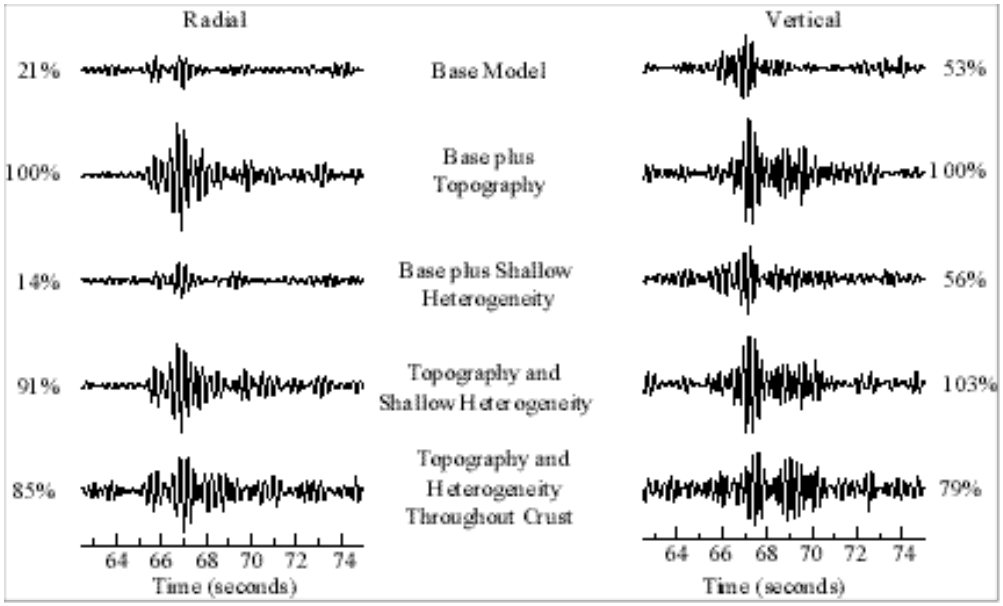

Figure 4. Radial (left) and vertical (right) component Lg (3.6 to 3.0 km/s) at 225 km for each of the models. All 5 traces are plotted at the same scale. Percentages to the left of each radial and right of each vertical trace are rms amplitudes as a percent of the radial and vertical records' rms amplitudes respectively for the homogeneous base model with topography added.

Figure 5 illustrates how broken up the pS wavefront is in the model with topography (lower row), compared with the flat-layered base model (upper row). It shows snapshots of the curl of the velocity, which isolates the shear waves, specifically the pS phase, shortly after the explosion. The source is at 325 meters below the free surface, in the horizontal center of the snapshots.

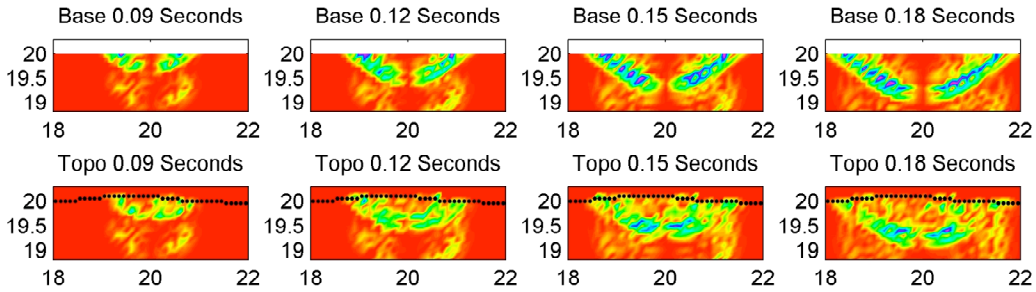

Figure 5. Snapshots of the curl of the velocity just after the explosion, for the homogeneous base model (top row) and model with topography (bottom row) illustrate the effect of topography on pS. The black line in the lower row shows the free surface.

The S* mechanism predicts conversion of P to S waves from sources within a small fraction of the wavelength from the surface as a result of curvature of the P wavefront (e.g., Vogfjord, 1997). Degelen sources were largely between 100 and 300 m depth. The source depth for all the synthetics shown in Figures 3 and 4 is 325 m. Figure 6 shows the dependence of S-phase amplitudes on source depth relative to wavelength, using wavenumber synthetics. They show large S amplitudes, arriving at approximately 64 seconds, for source depths less than 20% of the wavelength, and virtually no S for source depths near the wavelength. The record for the 300-m source depth, filtered from 3–5 Hz, has a small but clear S phase. This suggests that some, or perhaps most, of the Lg in the base model synthetics of Figures 3 and 4 is a result of S*.

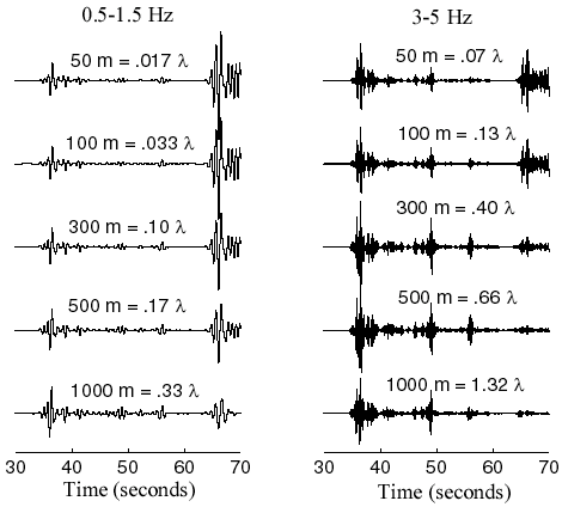

Figure 6. Wavenumber synthetics, at 225 km, for the homogeneous model at 1 (left) and 4 Hz (right), for sources at 50, 100, 300, 500, and 1,000 m. S* arrives at approximately 64 seconds.

Although S* appears to be a significant source of Lg, it predicts a strong depth dependence which has not been observed in Lg from explosions. It could, however, contribute to the relative increase in low frequency Lg, which has been observed in explosion-generated Lg. The scattering results shown in Figures 3-6 indicate that even in a high-velocity source medium where pS should not contribute to Lg, topographic scattering can trap more Lg than is produced by S*, at least at high frequency. One set of future finite-difference source calculations will use deeper point-explosion sources to eliminate the S* phase and so isolate just the scattering effects. A second set of calculations will use a CLVD source in the different models as a proxy for the nonspherical source effects, which will permit estimation of the Lg contribution from direct source generation.

Effects of topography and heterogeneity on Rg-to-Lg scattering: The finite-difference scattering calculations described above were also used to analyze Rg-to-Lg scattering. As with pS, the most significant scattering effect among the models is due to topography, and we focus on the difference in Rg scattering between the homogeneous plane-layered model and that same model plus the topography at Degelen.

Figure 7 shows the seismograms filtered in different passbands at 10 (left) and 30 (right) km from the source for the two plane-layered homogeneous models, flat and with topography. Each pair is plotted on the same scale. All records are plotted from 7.5 to 1.67 km/s group velocity. There is little effect below 1 Hz, the greatest difference being in amplitude, with the topographic model producing larger Rg. At 1–2 Hz, there are differences in arrival time, decay, and initial amplitude. The record for the topographic model is delayed, initially larger, and decays faster. There is also more P coda, which is most apparent at 30 km. At 2–4 Hz, there is practically no overlap in time between the well-defined Rg of the flat model, and the scattered Rg of the topographic model, even at 10 km. At 10 km, the topographic model Rg is larger, but by 30 km the Rg has slightly smaller maximum amplitude than that of the flat model, although it persists for much longer. At 4–8 Hz, Rg is not clearly distinguishable from coda in the topographic model.

To examine further what Rg scatters to, we look at cross sections of the vertical velocity and the curl, centered on the Rg phase near the source (Figure 8). This provides insight into the potential contribution of topographically scattered Rg to Lg. The vertical velocities (Figure 8, left half) show a compact Rg phase in the model without topography, but in the model with topography, the Rg energy has been spread out all along the surface. The downgoing phase in the cross sections at 1 second is P-to-S scattered energy. The curl of the velocities (Figure 8, right half), which isolates the shear waves, shows a similar result. At least during the first three seconds shown here, the main effect of topography on Rg is to cause strong dispersion of the phase rather than scattering into downgoing S.

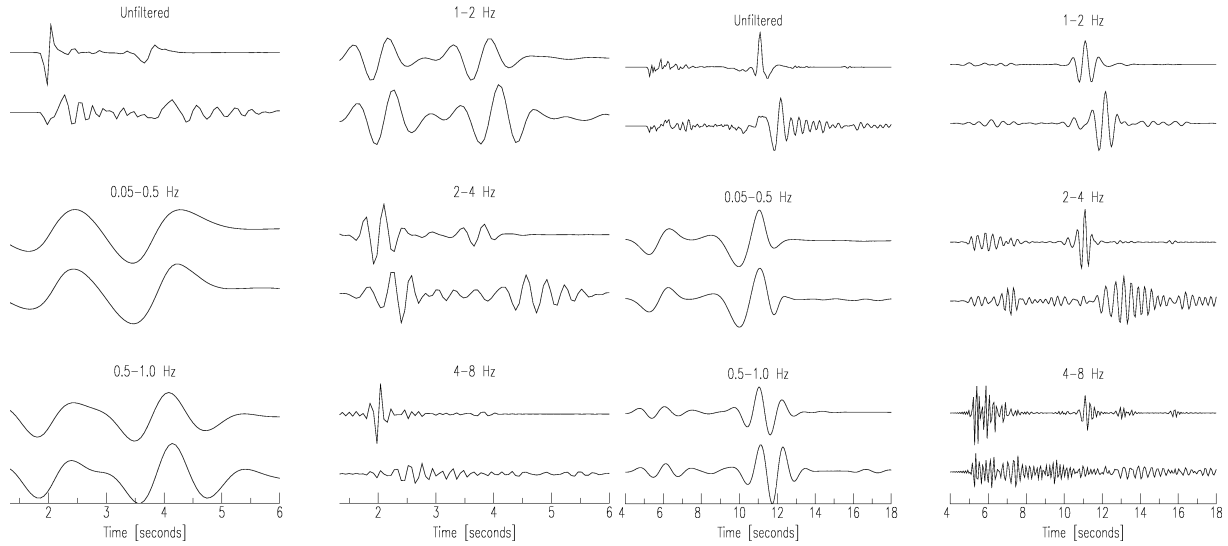

Figure 7. Synthetic seismograms, in various passbands, 10 (left half) and 30 (right half) km from the source, for the homogeneous model without (upper trace of pairs) and with (lower traces) topography.

To further quantify the effect of topography on Rg, we estimate Q as a function of frequency for the homogeneous model with a flat free surface and for the similar model with topography. A decrease in Q in the second model can be attributed to topographic scattering. The left side of Figure 9 shows frequency vs the estimated intrinsic Q values. The Q values determined for the base model are consistent with those of the original model structure (the frequency dependence is caused by the particular implementation of attenuation in the finite-difference calculation). Attenuation is greater for the model with topography (Figure 9, left side, and Table 3). The effect of dispersion is less than the measurement error for the model without topography but is dramatic for the model with topography. There the Rg is slowed at all frequencies, considerably at higher frequencies. This 2D analysis predicts that around 3 to 4 Hz, the scattering Q for Rg as a result of the topography at the Degelen test site is approximately 300. Around 1 Hz it is close to 1,000. A preliminary analysis of local Rg records from Degelen explosions indicates a significantly lower Q value. We cannot determine the partition between intrinsic Q and scattering Q in the observations, but the observations suggest that the scattering calculations probably underestimate the attenuation because of scattering. In the next section of this paper, we use a modal approach to determine an upper bound on Lg scattered from Rg.

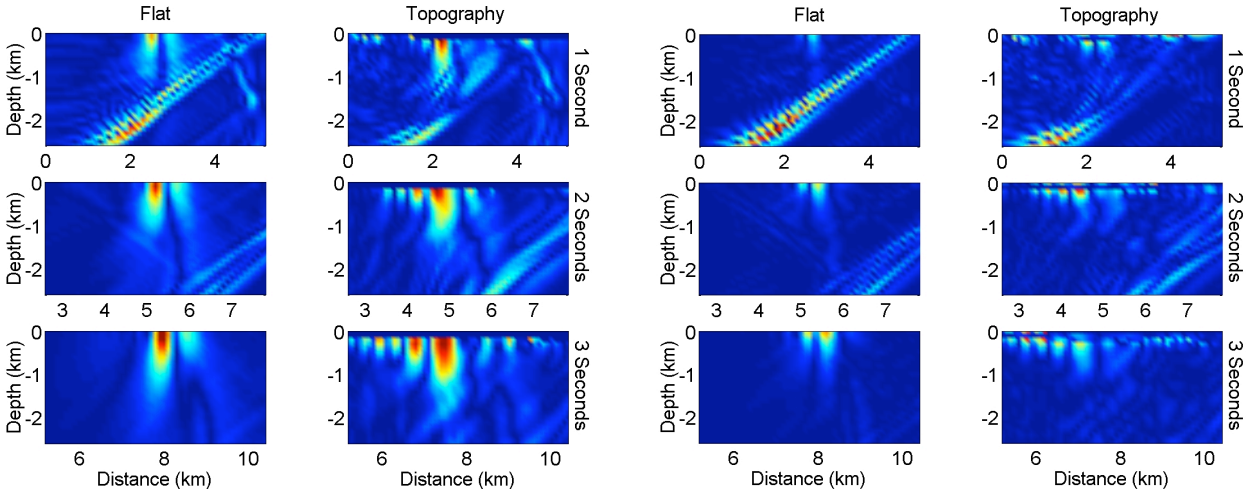

Figure 8. Cross sections of vertical velocity (left) and curl (right) centered on Rg at 1, 2, and 3 seconds for the homogeneous base model with a flat free surface (left column in each set of plots) and the same model plus topography (right column in each set of plots). Each pair (same time, different models) is plotted with the same color axis.

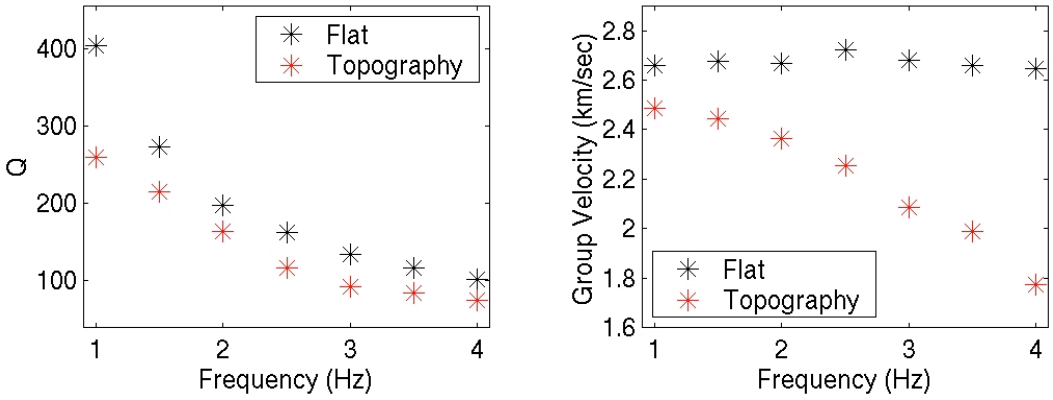

Figure 9. Q vs frequency (left) and group velocity vs frequency (right) for the flat (black) and topographic (red) models.

Table 3. Theoretical (subscript "model") and measured attenuation, Q, and group velocity, U, for the models without (Q_{flat} and U_{flat}) and with topography (Q_{topo} and U_{topo}). Scattering Q, Q_s, is determined by the difference in Q between models.

Passband (Hz)	Q_{model}	Q_{flat}	Q_{topo}	Q_s	U_{model}	U_{flat}	U_{topo}
0.5 - 1.5	502	404	260	730	2.66	2.66	2.49
1.0 – 2.0	294	274	215	1007	2.72	2.67	2.44
1.5 - 2.5	219	198	164	956	2.76	2.67	2.36
2.0 – 3.0	174	163	117	417	2.77	2.72	2.25
2.5 – 3.5	145	134	92	292	2.77	2.68	2.09
3.0 – 4.0	124	117	84	294	2.77	2.66	1.99
3.5 – 4.5	108	101	75	287	2.78	2.65	1.77

A modal method for calculating an upper bound on Rg-to-Lg scattering: To make a seismogram that approximates Lg generated by Rg scattering, we use energy conservation and the distribution of energy in each mode, derived from a similar analysis by Bennett et al. (1997). Rg is the fundamental mode surface wave generated by the explosion source. As discussed earlier, the explosion source can be complex, but can be represented to first order as a point explosion source plus a CLVD. For deeply overburied or decoupled explosions, the point source may be a very good approximation, but for shallower sources, the nonspherical components are important. We can make an approximate, but fairly realistic, calculation of the Lg generated by Rg by considering the Lg to be generated by scatterers at the earth's surface distributed over the region through which Rg propagates and assuming that all Rg converts to Lg. For this estimate, we make the following assumptions:

1) The explosion is a simple point explosion source. The same technique will work for a more complex explosion source.

2) Scattering occurs quickly enough that we can model the scattering duration as instantaneous. Under this assumption, we can also neglect intrinsic attenuation of the fundamental mode prior to scattering.

3) No energy is lost in scattering, and all scattering is forward scattering.

4) All scattering is from Rg to higher modes. We neglect secondary scattering and scattering to leaky phases.

5) The scattered energy has the modal distribution of a vertical point force. This is reasonable because the strongest Rg scattering occurs at the earth's surface.

We therefore consider that the scattered Rg consists of waves from a cylindrical distribution of point forces at the location of the propagating Rg phase, and that the scattered Rg goes into higher modes. These are very optimistic assumptions and should be regarded as providing an upper bound on Lg generated by Rg scattering. Forward

scattering is a better approximation than it may seem because scattering from a vertical point force in another direction simply adds to the outgoing wave in that direction with a small time delay.

Seismograms for Lg generated by the point explosion source, and by Rg scattering made under the assumptions listed above are shown in Figure 10 (left) for an 80-kiloton explosion at 500 meters depth in an earth model for NTS. The corresponding spectra are shown in Figure 10 (right). Figure 11 shows the spectra of the two time windows, 3.6 to 3.0 km/s and 3.0 to 2.5 km/s. The Lg from scattered Rg, at least in this optimal case, is comparable to Lg from the point explosion for frequencies of about 0.6 to 1 Hz, larger for lower frequencies, and smaller for higher frequencies. The Lg produced by scattered Rg has stronger excitation of the first higher mode than the Lg generated by the point explosion, which causes the higher spectral amplitudes at low frequencies and the late arriving higher-amplitude waves in the time series.

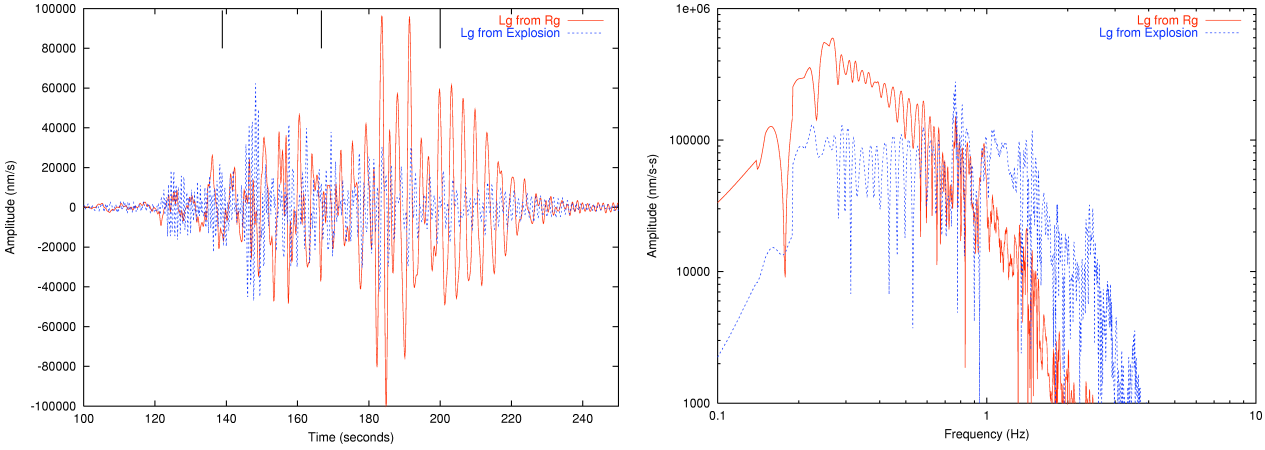

Figure 10. Left: Lg velocity seismograms calculated for a point explosion at 500 meters depth (blue) and for Lg generated by Rg scattered from the same explosion (red). Marks at the top show arrival times for 3.6, 3.0, and 2.5 km/s. Right: Lg spectra calculated from these two waveforms. The Lg calculated for the point explosion and that scattered from Rg have similar amplitudes within the 3.6 to 3.0 km/s group velocity window, but Rg scattering contributes more to the late Lg.

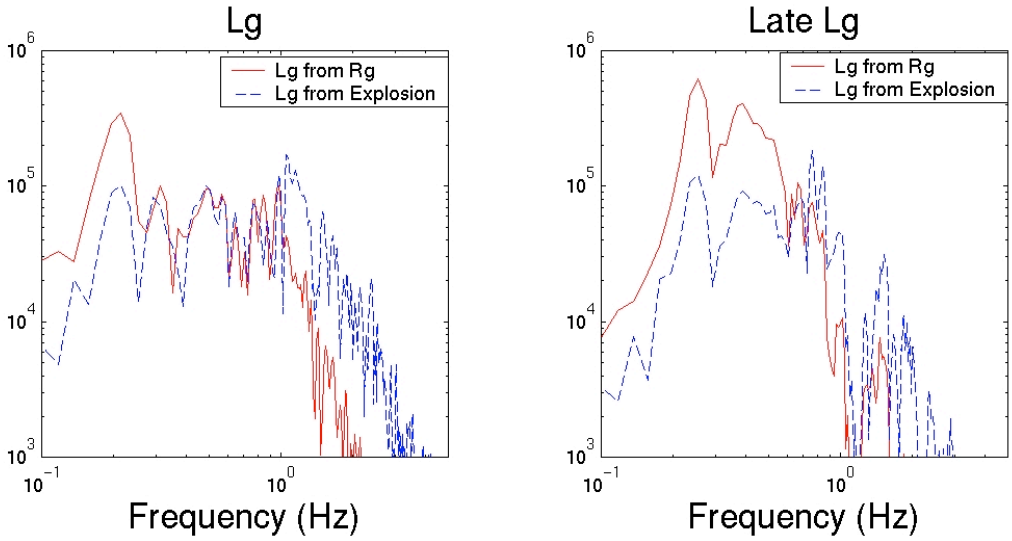

Figure 11. Spectra derived from the time series of Figure 10 using time windows of 3.6 to 3.0 km/s (left) and 3.0 to 2.5 km/s (right). In the Lg window, spectral amplitudes below 1 Hz are similar, but the spectra of the Rg-to-Lg scattered Lg begins to drop off at a lower frequency than the spectra of Lg calculated for the point explosion source. Spectra of both share the same spectral nulls.

These results suggest that Lg observed from overburied explosions is likely to consist of a superposition of Lg generated by the point-explosion source and by Rg scattering, that each source may dominate in a different frequency band, and that the two sources may interfere with each other, particularly near 1 Hz, complicating the use of the Lg waveform in discrimination. Explosions that are normally buried or underburied may have additional Lg as a result of direct generation of shear waves by nonspherical components of the source. Those components of the source will also generate more Rg. Future work will include more complex sources than a point explosion.

CONCLUSIONS AND RECOMMENDATIONS

We have investigated the most significant mechanisms for generating shear waves from explosions; P-to-S scattering, particularly from the free surface, Rg-to-Lg scattering, and direct generation of shear waves by nonspherical components of the explosion source. We have performed calculations capable of quantifying the contribution of each mechanism under different source and near-source propagation conditions, including depth, scaled depth, material properties, velocity structure, and topography. Nonlinear source calculations quantify the direct generation of shear waves. Finite-difference calculations provide insight into how scattering may trap P-to-S converted energy, particularly in high-velocity source media. They also provide insight into the nature of Rg scattering. A modal method of simulating Rg-to-Lg scattering places bounds on the Lg amplitude and characterizes its nature.

Specific results include the prediction of vertical and radial Lg and Sn for Degelen explosions by direct generation of S-waves by nonspherical components of the source and the prediction of vertical and radial Lg for the NPE explosion by free surface P-to-S-scattered waves. Topography at Degelen has a much stronger effect than 5% standard-deviation velocity heterogeneities on pS, randomizing its incidence so that more pS is trapped in the crust as Lg. Topography also more strongly scatters and disperses Rg than do the crustal heterogeneities tested. The scattered and dispersed Rg energy appears to remain concentrated along the surface. Modal calculations indicate that if all Rg scatters to Lg, its contribution is predominantly to late Lg and lower frequencies.

Recommended future work should include further comparison of simulations with data from the extensive data set summarized in Table 2. For example, we intend to perform further nonlinear finite difference simulations of the explosion source to predict near regional and regional data from Degelen and Balapan explosions to isolate the direct contribution of the source to the regional waveforms, distinct from near-source and path-scattering effects. We also intend to model the Rg-to-Lg scattering mechanism using the time-dependent modal energy transfer technique for several realistic structures, including Central Asia and NTS, and make a quantitative estimate of the contribution of Rg scattering to Lg. We will compare characteristics of jointly observed Lg and Rg in Eurasian explosions and NTS to determine whether predictions and observations are consistent. This will include the comparison of spectral characteristics of near-regional and regional Lg with predictions based on source calculations and Rg scattering calculations, taking into account the source-region structure, near-regional path characteristics, source depth, scaled depth, and yield.

Future data analysis and calculations with the methods presented will also focus on subsets of events for which only one parameter, such as depth, changes. Future work must also address the question of tangential Lg and Sn, which is not well explained by current mechanisms. We will extend the scattering calculations to 3D, both to more realistically quantify the effects of topography and heterogeneity and to investigate the randomization of shear-wave polarization.

REFERENCES

Bennett, T. J., K. L. McLaughlin, M. Marshall, and J. L. Stevens (1997), "The Physical Basis for the Lg/P Discriminant: General Properties and Preliminary Modeling," PL-TR-97-2044, MFD-FR-97-15727

Vogfjord, K. (1997), "Effects of Explosion Depth and Earth Structure on the Excitation of Lg Waves: S* Revisited," *Bull. Seism. Soc. Am.*, 87, 1100–1114